arXiv:0803.2655v2 [cond-mat.stat-mech] 16 Apr 2008

Entanglement in a periodic quench

Viktor Eisler* and Ingo Peschel

Fachbereich Physik, Freie Universität Berlin, Arnimallee 14, 14195 Berlin, Germany

We consider a chain of free electrons with periodically switched dimerization and study the entanglement entropy of a segment with the remainder of the system. We show that it evolves in a stepwise manner towards a value proportional to the length of the segment and displays in general slow oscillations. For particular quench periods and full dimerization an explicit solution is given. Relations to equilibrium lattice models are pointed out.

I. INTRODUCTION

Entanglement is a basic feature of non-trivial quantum states and has been studied extensively for the ground states of standard many-body systems [1]. However, the question how it evolves in time-dependent situations is equally interesting. The simplest case is a quench where the Hamiltonian is changed instantaneously from H_0 to H_1 and one follows the subsequent evolution of the initial state, usually taken to be the ground state of H_0. For global quenches, where a parameter is changed everywhere in the same way, it was found that in homogeneous chains the entanglement entropy S between a segment of length L and the remainder first increases linearly with time and then approaches an asymptotic value proportional to L [2, 3, 4, 5]. Thus the time evolution leads to a much larger entanglement than found in equilibrium where even for critical chains S is only proportional to $\ln L$. This result can be interpreted in a simple picture where pairs of quasiparticles establish the entanglement between the two parts of the system [2]. Alternatively, the time-dependent state may be viewed as the ground state of an evolving Hamiltonian which is strongly non-local and gives long-ranged correlations.

In this paper we will study a more general situation and consider not a single quench, but a periodic sequence of changes $H_0 \leftrightarrow H_1$ and its effect on the entanglement entropy. Such periodic changes have been considered in some papers on Ising chains kicked by a transverse [6, 7, 8] or a tilted field [7, 9, 10]. We will investigate a system of free electrons hopping on a chain with alternating bonds. The corresponding dimerization parameter is then switched between the values $\pm\delta$, which simply interchanges weak and strong bonds. Although there is a mapping to the transverse Ising chain, the hopping model has a more direct physical significance since it could be

---

[*] Corresponding author E-mail: `eisler@physik.fu-berlin.de`

realized with optical lattices. There have already been experiments with dilute gases where periodic potentials were applied in the form of kicks [11]. Other experiments [12, 13] have motivated studies of chains where the parameters in the Hamiltonian were assumed to vary harmonically. In this case, however, the focus was either on the energy absorption [14, 15, 16] or on work fluctuations [17].

The periodic quench has some important general features. In the evolution, one can distinguish what happens after full quench periods and what happens at the times in between. This situation is analogous to the case of a particle moving in a periodic potential and has been discussed extensively for simple kicked quantum systems [18]. For a full quench period, the time evolution operator is the product of two exponentials and analogous to the transfer matrix in a classical two-dimensional system with a layered structure. One can write it as a single exponential with a certain effective Hamiltonian. The formulae are very similar to those one finds for the Ising model on a square lattice. They also show that the effective Hamiltonian is critical if, as we assume, H_0 and H_1 act for the same length of time. Compared to a simple critical quench, however, one has the additional evolution during the intermediate times. The unitarity of the discrete evolution from period to period, on the other hand, leads to effects not present in models with Euclidian time.

We describe the model and the method of computing S via correlation functions in Section 2. Then we treat in Section 3 the fully dimerized case $\delta = 1$ which is particularly simple. The time evolution can then be represented graphically and for special values of the quench period the particles even move with strictly uniform velocity. For $S(t)$ one finds a step structure and an asymptotic value proportional to L. We discuss the dependence on the quench period and show the behaviour for arbitrary times. Section 4 deals with arbitrary dimerization. Here the quasiparticles in the effective Hamiltonian can have a more complicated dispersion in which case additional slow oscillations appear in the entanglement entropy. In Section 5 we sum up our findings and in the Appendix we give the formulae for calculating the correlation matrix in the general case.

II. MODEL AND METHOD

We will study a half-filled ring of free electrons with $2N$ sites and alternating hopping as shown in Fig. 1.

The Hamiltonian is

$$H = -J \sum_{m=1}^{N} \left(\frac{1+\delta}{2}\, c_{2m}^{\dagger} c_{2m+1} + \frac{1-\delta}{2}\, c_{2m+1}^{\dagger} c_{2m+2} + \text{h.c.} \right) \tag{1}$$

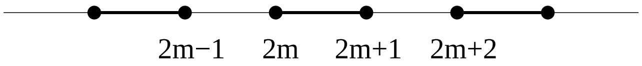

FIG. 1: Geometry of the dimerized hopping model.

and, up to boundary effects, also describes a dimerized XX spin model. In the following we set $J = 1$. The diagonal form of H is obtained by working with cells of two sites, defining $c_{2m} = a_m$, $c_{2m+1} = b_m$, and performing a Fourier transformation

$$\begin{pmatrix} a_m \\ b_m \end{pmatrix} = \frac{1}{\sqrt{N}} \sum_q \mathrm{e}^{iqm} \begin{pmatrix} a_q \\ b_q \end{pmatrix} \quad , \quad q = \frac{2\pi}{N} k \; . \tag{2}$$

Then

$$H = -\sum_q \omega_q (\alpha_q^\dagger \alpha_q - \beta_q^\dagger \beta_q) \tag{3}$$

where

$$\omega_q = \sqrt{\cos^2 \frac{q}{2} + \delta^2 \sin^2 \frac{q}{2}} \tag{4}$$

and the Fermi operators are related via

$$a_q = \frac{1}{\sqrt{2}} \mathrm{e}^{-i\varphi_q/2} (\alpha_q + \beta_q) \quad , \quad b_q = \frac{1}{\sqrt{2}} \mathrm{e}^{i\varphi_q/2} (\alpha_q - \beta_q) \tag{5}$$

with

$$\mathrm{e}^{i\varphi_q} = \mathrm{e}^{iq/2} \, \frac{\cos \frac{q}{2} - i\delta \sin \frac{q}{2}}{\omega_q} \; . \tag{6}$$

In the ground state, all α-levels are occupied and all β-levels are empty. The single-particle spectrum has a gap at $q = \pm\pi$ for all $\delta \neq 0$. For vanishing dimerization δ, (4) gives $\omega_q = \cos(q/2)$ which is the usual result for homogeneous hopping, but folded into the smaller Brillouin zone. For $\delta = 1$ the dispersion becomes flat, $\omega_q = 1$. A change $\delta \to -\delta$ does not affect ω_q which simplifies the situation in the quench.

At time $t = 0$, the system is taken to be in the ground state $|\Phi_0\rangle$ of $H_0 = H(\delta)$. The periodic quench consists of switches between H_0 and $H_1 = H(-\delta)$ at times $n\tau$ where $n = 0, 1, 2, \ldots$. This interchanges weak and strong bonds and forces the system to adapt. Formally, the wave function then evolves according to

$$|\Phi(t)\rangle = U(t) |\Phi_0\rangle \tag{7}$$

with a unitary operator $U(t)$ which for $t = n \cdot 2\tau$, i.e. after n full periods, is given by

$$U(2n\tau) = U^n \tag{8}$$

where

$$U = U_0\, U_1 = \mathrm{e}^{-iH_0\tau}\mathrm{e}^{-iH_1\tau} \tag{9}$$

describes the evolution over one period.

We are interested in the entanglement of a segment of L sites with the remainder of the system. The corresponding entanglement entropy S follows from the reduced density matrix ρ of the segment which has the form [19]

$$\rho = \frac{1}{Z}\, e^{-\mathcal{H}} \ , \quad \mathcal{H} = \sum_{k=1}^{L} \varepsilon_k(t) f_k^\dagger f_k \ . \tag{10}$$

Here Z is a normalization constant ensuring $\mathrm{Tr}\,\rho = 1$ and the fermionic operators f_k follow from the c_n by an orthogonal transformation. Then $S = -\mathrm{Tr}\,(\rho \ln \rho)$ is determined by the single-particle eigenvalues $\varepsilon_k(t)$ according to

$$S(t) = -\sum_k \zeta_k(t) \ln \zeta_k(t) - \sum_k (1 - \zeta_k(t)) \ln(1 - \zeta_k(t)) \tag{11}$$

where $\zeta_k(t) = 1/(\exp(\varepsilon_k(t)) + 1)$. The $\zeta_k(t)$ are the eigenvalues of the correlation matrix

$$C_{lm}(t) = \langle \Phi(t) | c_l^\dagger c_m | \Phi(t) \rangle = \langle \Phi_0 | c_l^\dagger(t) c_m(t) | \Phi_0 \rangle \tag{12}$$

restricted to the sites of the subsystem. To obtain $\mathbf{C}(t)$ one relates it to $\mathbf{C}(0)$ by expressing the Heisenberg operators $c_m(t) = U^\dagger(t) c_m U(t)$ as linear combinations of the c_j. For this, one has to diagonalize the operator U in (9) which is the product of two exponentials. This is a well-known problem which first appeared (without the factors of i) in the solution of the two-dimensional Ising model via transfer matrices [20]. A special case is treated in Section III while the general expressions for the elements of $\mathbf{C}(t)$ are given in the Appendix. Evaluating them numerically and diagonalizing the matrix one then finds the entropy.

One should note that there is a close relation between XY and transverse Ising (TI) chains [21, 22] which was recently extended to their entanglement properties [23, 24]. This means that the Hamiltonian H in (1) can be obtained by putting two TI models on alternating sites of a chain, performing a dual transformation and choosing the coupling constants λ_α and the fields h_α as $h_1 = \lambda_2 = (1 + \delta)/2$, $h_2 = \lambda_1 = (1 - \delta)/2$. Thus one TI model is in the ordered and the other in the disordered phase. Changing the sign of δ then switches each model to the opposite phase.

In the special case $\delta = \pm 1$ one has either only a field or only a nearest neighbour coupling. This corresponds to an Ising chain kicked periodically by a transverse field [6, 7, 8], because during the δ-pulses describing the kicks one can neglect the coupling terms. One could work in this TI formulation, but the dimerized chain provides a nicer physical picture as will be seen in the following section where we actually treat the case $\delta = 1$ before dealing with the general situation.

III. FULLY DIMERIZED CASE

In this section, we treat a periodic quench between $\delta = \pm 1$ which is particularly transparent and instructive. This situation has also been considered in [25] for bosons.

A. Time evolution operator

For $\delta = 1$, the system consists of independent pairs of sites. For each pair, the Hamiltonian has the form

$$h = -(a^\dagger b + b^\dagger a) \tag{13}$$

and is diagonalized by setting $a = (\alpha + \beta)/\sqrt{2}$, $b = (\alpha - \beta)/\sqrt{2}$. This corresponds to $\omega_q = 1$, $\varphi_q = 0$ in (4)–(6) and gives

$$h = -(\alpha^\dagger \alpha - \beta^\dagger \beta) \; . \tag{14}$$

The time dependence of a and b is then

$$\begin{pmatrix} a(t) \\ b(t) \end{pmatrix} = \begin{pmatrix} \cos t & i \sin t \\ i \sin t & \cos t \end{pmatrix} \begin{pmatrix} a \\ b \end{pmatrix} = v(t) \begin{pmatrix} a \\ b \end{pmatrix} \tag{15}$$

and the full evolution matrix has block form with N such v's along the diagonal. The same holds for the other half-period but then the pairs and thus the v's are shifted by one site. The complete time evolution can therefore be represented as in Fig. 2, where each shaded square corresponds to a matrix $v(\tau)$. Such a chequerboard structure also appears in the time evolution of lattice-gas models with parallel dynamics [26, 27, 28]. In equilibrium problems it is found for partition functions of vertex models oriented diagonally [29] or of one-dimensional quantum systems treated with a Trotter decomposition of $\exp(-\beta H)$ [30].

Using translational invariance, the $(2N \times 2N)$ matrix $\mathbf{V} = \mathbf{V}_0 \mathbf{V}_1$ for one period is found to have the eigenvalues $\exp(\pm i \gamma_q)$ where

$$\cos \gamma_q = \cos^2 \tau - \sin^2 \tau \cos q \; . \tag{16}$$

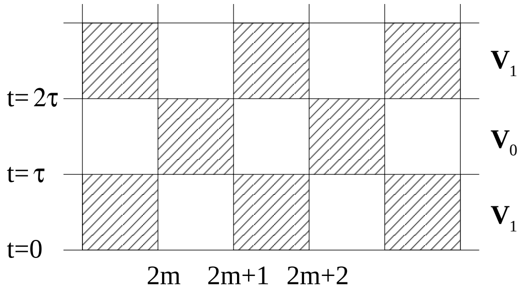

FIG. 2: Time-evolution pattern for full dimerization. The shaded squares indicate the coupling of the sites and of the corresponding Fermi operators in each half-period.

Therefore, writing the operator U in (9) as a single exponent

$$U = \mathrm{e}^{-i\bar{H}2\tau} \tag{17}$$

the diagonal form of the effective Hamiltonian is

$$\bar{H} = \sum_q \nu_q(\xi_q^\dagger \xi_q - \eta_q^\dagger \eta_q) \tag{18}$$

where $\nu_q = \gamma_q/2\tau$ and the Fermi operators ξ_q, η_q follow from the eigenvectors of $\mathbf{V}$.

The single-particle energies of $\bar{H}$ are shown in Fig. 3 for several values of τ. The main feature is that the spectrum is always gapless at $q = \pm\pi$. Thus the evolution over one period is given by a critical Hamiltonian. This is a consequence of the symmetry of the two half-periods. If they have different lengths τ_0, τ_1, Eq. (16) is changed to

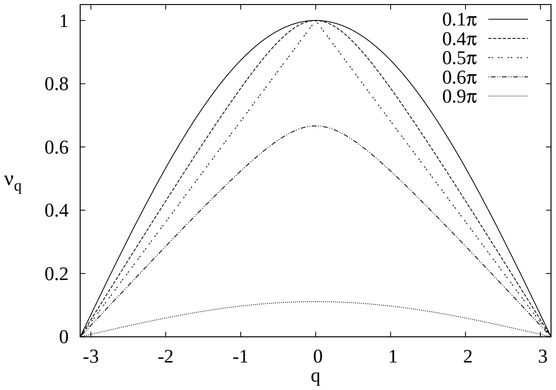

FIG. 3: Dispersion of the single-particle excitations in $\bar{H}$ for five values of the half-period τ.

$$\cos\gamma_q = \cos\tau_0 \cos\tau_1 - \sin\tau_0 \sin\tau_1 \cos q \tag{19}$$

and $\gamma_\pi = |\tau_0 - \tau_1|$. One should note that the relation (19) is the trigonometric analogue of the hyperbolic formula

$$\cosh\gamma_q = \cosh 2K_1^* \cosh 2K_2 - \sinh 2K_1^* \sinh 2K_2 \cos q \tag{20}$$

found for the row transfer matrix of the two-dimensional Ising model on a square lattice with couplings K_1 and K_2 [20]. The quantity K_1^* in (20) is the dual coupling of K_1, $\tanh K_1^* = \exp(-2K_1)$. This illustrates the close connection between the two problems mentioned earlier.

B. Hamiltonian limit

For rapid switching, $\tau \ll 1$, one finds from (16) $\gamma_q = 2\tau\cos\frac{q}{2}$, i.e. $\nu_q = \cos\frac{q}{2}$. According to (4) these are the single-particle energies ω_q of H in the absence of dimerization. This is not surprising since for $\tau \ll 1$ one can write directly

$$U = \mathrm{e}^{-iH_0\tau}\mathrm{e}^{-iH_1\tau} \approx \mathrm{e}^{-i(H_0+H_1)\tau} \tag{21}$$

which gives $\bar{H} = (H_0 + H_1)/2 = H(\delta = 0)$. Therefore the evolution for times $t = n \cdot 2\tau$ is the same as for a single quench to a homogeneous hopping model. This situation has already been studied in [31], Appendix B, where the correlation matrix $\mathbf{C}(t)$ was calculated and the entanglement entropy was found to approach the asymptotic value

$$S(\infty) = L\,(2\ln 2 - 1) \tag{22}$$

for large L.

C. The special case $\tau = \pi/2$

For this value of τ, $\nu_q = 1 \pm q/\pi$ is strictly linear and describes massless particles with velocity $v = 2/\pi$ in units of the lattice spacing. This can also be seen directly in real space. According to (15), one has

$$a(\frac{\pi}{2}) = ib \quad , \quad b(\frac{\pi}{2}) = ia \tag{23}$$

such that particles in a cell interchange positions. This continues in subsequent half-periods and leads to straight paths as sketched in Fig. 4.

A correlation which exists initially between the first neighbours A and B is thereby extended to third neighbours in the first step, to fifth neighbours in the second one and so forth. This

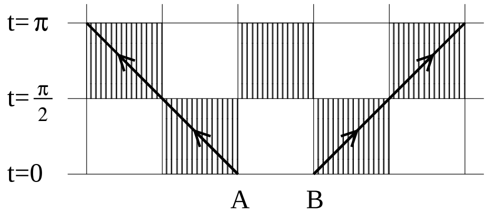

FIG. 4: Motion of the particles for $\tau = \pi/2$.

permits to set up the correlation matrix $\mathbf{C}(t)$. If A and B form a cell, then in the ground state all correlation functions are equal

$$\langle a^\dagger a\rangle = \langle a^\dagger b\rangle = \langle b^\dagger a\rangle = \langle b^\dagger b\rangle = \frac{1}{2} \tag{24}$$

and the same holds then for correlated sites at later times. For the entanglement entropy only those correlations are relevant which connect sites inside and outside the subsystem. They lead to an eigenvalue $\zeta = 1/2$ which gives a contribution of $\ln 2$ to S. It is not difficult to see that in one step the number of in-out correlations does not change while in the other one it increases by 4. Thus in a full period

$$\Delta S = 4 \ln 2 \tag{25}$$

and the increase continues until S reaches the highest possible value $L \ln 2$. This build-up of the entanglement is an exact lattice realization of the light-cone picture introduced by Calabrese and Cardy [2] in the context of single quenches and analyzed further in [32, 33].

The description becomes complete if one also looks at intermediate times. By studying small values of L one finds that during the half-period where S changes, the correlation matrix has non-trivial eigenvalues $\zeta_1 = \sin^2(t/2)$ and $\zeta_2 = \cos^2(t/2)$. With (11) these give a contribution

$$\Delta S(t) = -4\left[\sin^2\frac{t}{2}\ln\sin^2\frac{t}{2} + \cos^2\frac{t}{2}\ln\cos^2\frac{t}{2}\right] \tag{26}$$

which describes the increase by $4\ln 2$ between $t = 0$ and $t = \pi/2$. Therefore $S(t)$ has a step-like structure where plateaus are connected by the function $\Delta S(t)$. The result of a numerical calculation for $L = 20$ is shown in Fig. 5. Due to the alternating structure of the chain, there are two possible choices for the subsystem if L is even. It may contain initially $L/2$ complete cells, in which case it is uncorrelated with the surrounding and $S(0) = 0$. Or it contains only half a cell at each end, which contributes $\ln 2$ to the entanglement giving altogether $S(0) = 2\ln 2$. This leads to the two curves in the figure. Note that for the second choice the last plateau is absent and the final step has only height $2\ln 2$. Its form is also slightly modified. The inset shows a comparison of $\Delta S(t)$ with the analytical formula (26).

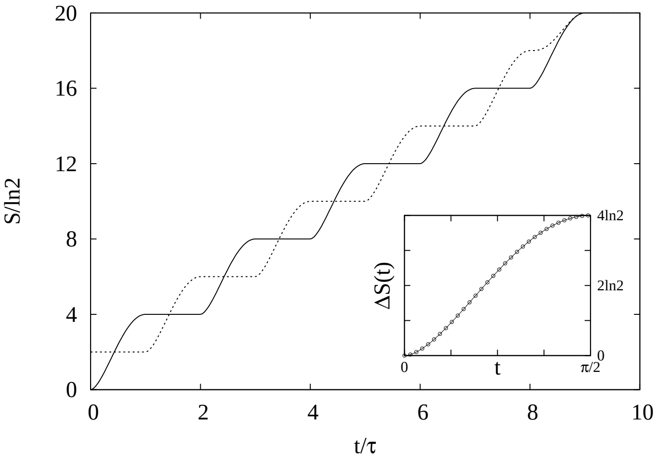

FIG. 5: Entanglement entropy $S(t)$ for $\tau = \pi/2$, $L = 20$ and the two choices of the subsystem, see text. Inset : Enlarged view of the ascending part $\Delta S(t)$. The line is the analytical result.

These considerations can also be extended immediately to times τ which are multiples of $\pi/2$. Then the particles change their position in the cells several times during one half-period. Consequently, the plateaus are longer and $S(t)$ follows the function (26) for a longer interval. Thus if $\tau = (2k+1)\pi/2$ the plateaus are connected by an oscillating function. Such a case is also discussed below for more general times. On the other hand, if τ is an even multiple of $\pi/2$, the oscillations always lead back to the initial value of S and there is no systematic ascent.

D. General times τ

For general values of the quench period, no analytical treatment is possible and the entropy has to be obtained numerically as described in Section 2. Figure 6 shows results for small values of τ on the left and for larger ones on the right.

The overall behaviour is an initial, on average linear increase followed by a sharp bend and a final approach to an asymptotic value. The upper bound $L\ln 2$ is only reached for $\tau = \pi/2$. The bending points can be related to the velocity of the fastest one-particle excitations in the effective Hamiltonian. This is given by

$$v_{\max} = 2\left|\frac{\partial \nu_q}{\partial q}\right|_{q=\pi} = \frac{\sin\tau}{\tau} \qquad (27)$$

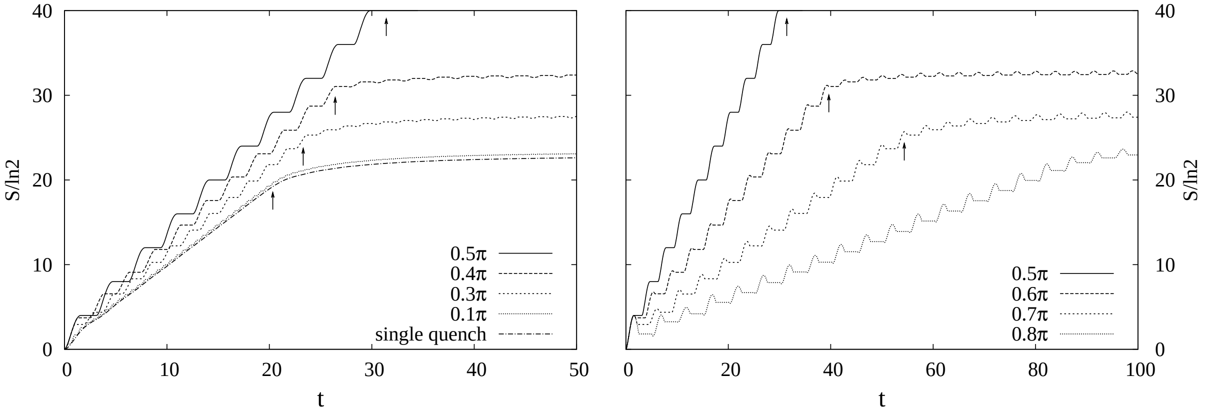

FIG. 6: Entanglement entropy $S(t)$ for $L = 40$ and different values of τ. Left: Small τ. Right: Larger τ. The arrows indicate the times $L/2v_{\max}$.

where the factor of 2 is needed for the distance to be measured in sites instead of cells. Then the time required for these excitation to travel from the middle of the block to the surrounding is given by $L/2v_{\max}$. The corresponding values are indicated by arrows in Fig. 6 and locate the cross-over points very well. In the Hamiltonian limit $\tau \to 0$, the result for the single quench to the homogeneous chain is recovered.

Let us now discuss the fine structure of the curves. First of all, the increase takes place in steps with well defined plateaus. These plateaus still occur because in one of the two half-periods the time evolution in the subsystem is decoupled from that in the surrounding. Thus the entanglement cannot change. For small τ, the plateaus are connected by simple monotonous curves, but for larger periods, an overshooting occurs which turns into an oscillation for even larger τ. A particle then performs more than one cycle in a cell before the next switching occurs. This case is shown in more detail in Fig. 7 for $\tau = 1.7\pi$. The first oscillation is given by the function (26) up to the time $t = \tau$ when the plateau starts. The next oscillations look similar but their amplitudes are not the same and even after a rescaling there remain small differences. In fact, their similarity is even somewhat surprising. On the right of Fig. 7 the non-trivial eigenvalues ζ_k which determine the variation of $S(t)$ are plotted. One sees that only one such eigenvalue (and its partner $1 - \zeta_k$) exists in the beginning but that more and more appear in later periods and contribute to S. Thus one expects differences in the functional form.

Looking at the step heights in Fig. 7, one sees that they are not all equal. This is a general feature and illustrated in Fig. 8. The main graph shows the step height ΔS_n of the n-th step for the initial increase of $S(t)$ with the average value subtracted. It is an oscillatory decaying function

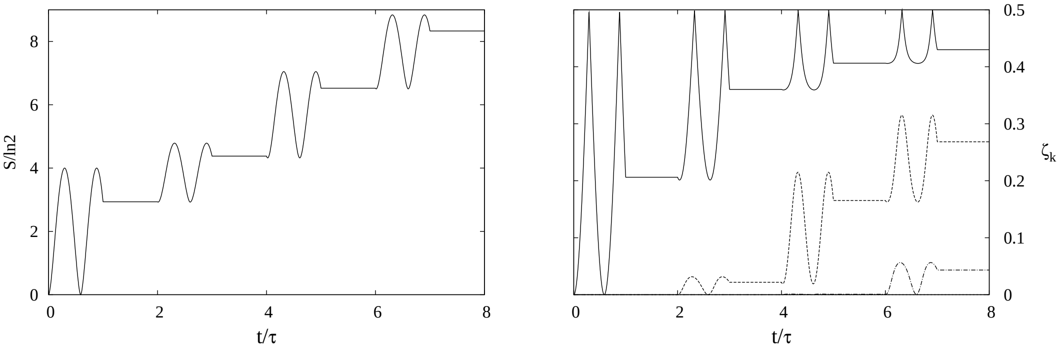

FIG. 7: Left: Entanglement entropy for $S(t)$ for $L = 40$ and $\tau = 1.7\pi$. Right: The eigenvalues $\zeta_k(t)$ producing $S(t)$.

independent of L and can be very well described by the expression

$$\Delta S_n = \Delta S_0 + A\frac{\sin(4\tau n - \varphi)}{n^{3/2}} \tag{28}$$

with an amplitude A and a phase φ.

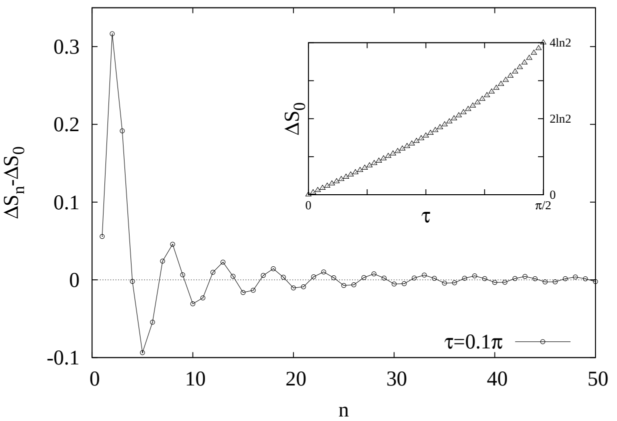

FIG. 8: Variation of the step height in $S(t)$ for $L = 200$ and $\tau = 0.1\pi$. The average value ΔS_0 is subtracted. Inset: ΔS_0 as a function of τ.

This result is easy to understand if one takes into account that the integrals (39) for the elements of the correlation matrix contain the number of the period in the form of factors $\sin(2\gamma_q n)$ and $\cos(2\gamma_q n)$ and that the main contribution comes from the region near $q = 0$ where the dispersion curve has its maximum. This gives oscillations in n with frequency $2\gamma_0 = 4\tau$ which persist in $S(t)$. Moreover, the density of states in the integration leads to a dependence $1/n^{3/2}$, which was also found in a previous treatment of the Hamiltonian limit [31] and in a calculation of a related TI correlation function [6]. The oscillations go away if either $\tau = 0$ or $\tau = \pi/2$. Between these two limits, the average step height increases monotonously from zero to $4\ln 2$ as shown in the inset of the Figure. Thus the case $\tau = \pi/2$ studied in the last subsection has not only regular steps but also the highest ones and thus leads to the fastest increase of S. Since the dispersion relation γ_q is invariant under $\tau \to \pi - \tau$ and under $\tau \to \tau + k\pi$, one can use the above results to obtain the step heights for arbitrary periods.

In the region beyond the cross-over point at time $L/2v_{\text{max}}$ the step height decays rapidly towards zero with the same $n^{-3/2}$ power law for large n as before and one can still observe the same oscillations.

IV. PARTIALLY DIMERIZED CASE

We now turn to the case of general values $\delta < 1$, where the system has alternating weak and strong hopping. Results for a short quench time, $\tau = 0.4\pi$, are shown in Fig. 9. The curves resemble those in Fig. 6, but there is one basic difference. Since the cells are always coupled, one does not have plateaus any more. Instead, $S(t)$ increases slowly during those half-periods where the plateaus occur for $\delta = 1$ and faster for the others. Together this still gives a kind of step structure, but the steps are washed out. As δ becomes smaller, the differences between the two half-periods also become smaller and the curve smoothens more and more. At the same time the average slope decreases. Moreover, the initial value $S(0)$ is non-zero and becomes larger, approaching the value $S = 1/3 \ln L + k$ of the homogeneous chain. The oscillations with the quench period persist also beyond the bending point and decrease there with δ in the same way.

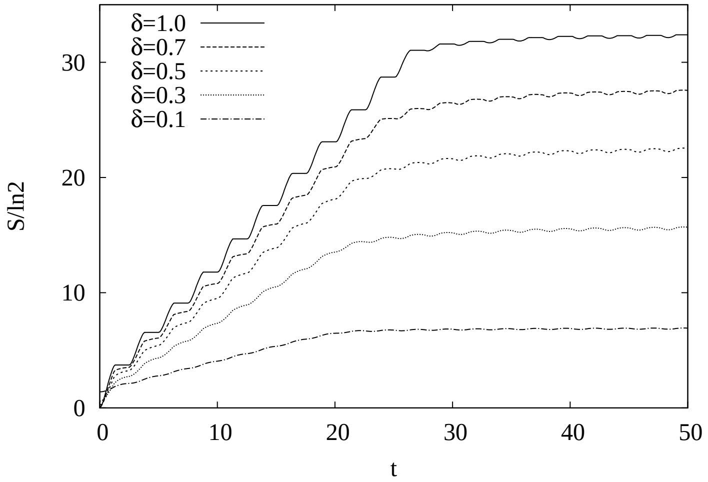

FIG. 9: Entanglement entropy for $L = 40$ and $\tau = 0.4\pi$ for five values of the dimerization δ.

This might suggest that the behaviour of S becomes less interesting for partial dimerization. However, this is not true. In Fig. 10 we show results for a larger quench time, $\tau = 0.7\pi$ and several values of δ below 0.5. In addition to small and fast oscillations one now observes very slow ones with rather large amplitudes and a frequency which decreases with δ. As in the previous section, the origin of these oscillations can be found in the dispersion curve for γ_q. In Fig. 11 we have plotted γ_q given by Eqs. (32) and (33) in the Appendix as a function of δ. One sees that while there is a single maximum at $q = 0$ for large δ, a double-peak structure develops below $\delta = 0.7$ and the maxima approach the zone boundary at π for $\delta \to 0$. The reason is that for small δ the factor $\cos(\varphi_1 - \varphi_0)$ is almost constant and γ_q is basically determined by ω_q in the trigonometric functions. For $\delta = 0$ one finds exactly $\gamma_q = 2\tau\cos(q/2)$ which gives the uppermost curve in the figure when folded into the first Brillouin zone.

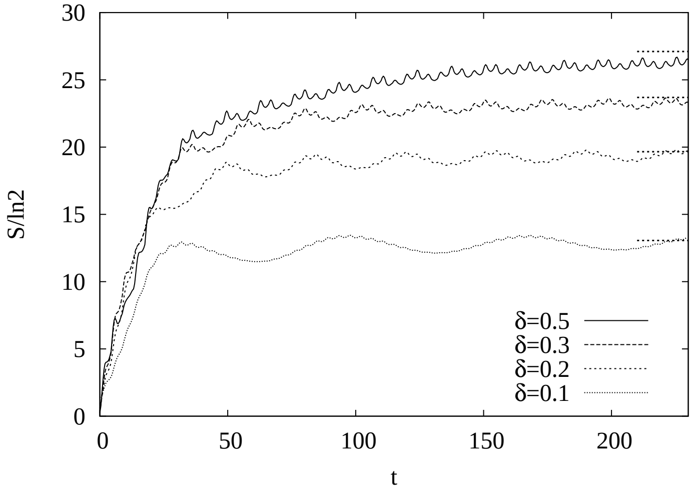

FIG. 10: Entanglement entropy for $L = 40$ and $\tau = 0.7\pi$ for several values of the dimerization δ. The dotted lines on the right indicate the asymptotic values.

Writing $\gamma_{\text{max}} = \pi - \Delta$, the maxima lead to a long-time behaviour of the correlations of the form

$$\cos(2n\gamma_{\text{max}}) = \cos(2n(\pi - \Delta)) = \cos(2n\Delta) \tag{29}$$

and thus to oscillations with frequency 2Δ. The effect is the same as in Section III for the case τ near $\pi/2$ and may be called an Umklapp effect in the frequency space due to the discrete times. The double-peak structure in the dispersion can also lead to beats in $S(t)$, if the two frequencies at the maximum and the minimum are close to each other. Such phenomena have also been observed in [7].

Finally, we show in Fig. 12 how the asymptotic value of S depends on the parameters τ and

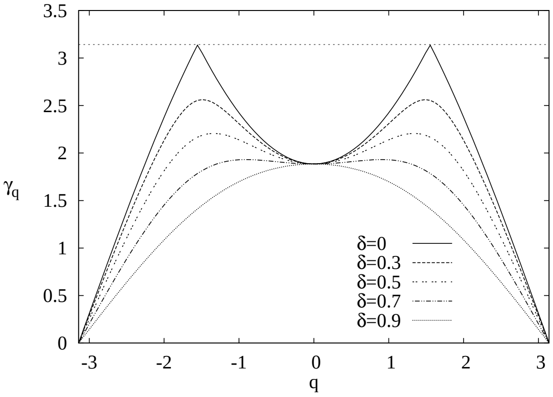

FIG. 11: Dispersion γ_q for $\tau = 0.7\pi$ and several values of the dimerization.

δ. The calculation uses the expressions (41) in the Appendix for the elements of the correlation matrix which is then diagonalized. In all cases, $S(\infty)$ is proportional to L. In the fully dimerized case, it is a periodic function of τ with period π and maxima at odd multiples of $\pi/2$. The latter times still play a special role for partial dimerization because the maximal value of ω_q is always 1, but $S(\infty)$ has only steps there. In general, it decreases as one lowers δ, which is reasonable, as then the changes during the quench become smaller. For $\delta = 0$, there is no change at all and S has to be constant in time and non-extensive. One should note that the asymptotic values give no information on how fast they are reached. An extreme case is $\delta = 1$ and τ near $k\pi$. Then the approach is very slow and if τ equals $k\pi$ exactly, S remains at its initial value apart from periodic excursions as noted in Section III.

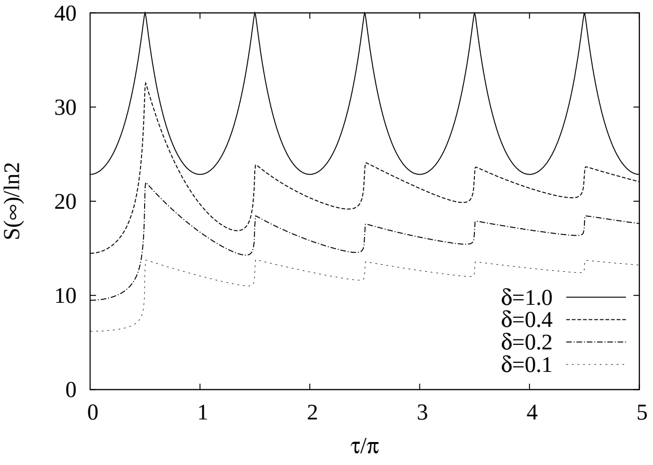

FIG. 12: Asymptotic value of the entanglement entropy for $L = 40$ as a function of the quench period for different dimerizations.

V. SUMMARY AND CONCLUSION

We have studied an integrable quantum chain under the influence of a periodic quench. Because one switches back and forth between the two equivalent broken-symmetry arrangements, the time evolution is on average that of a translationally invariant system. The entanglement was studied via the entropy S for a segment of L sites. This contains more information than the Q measure related to reduced single-site density matrices and used in [7]. We found an overall behaviour similar to that in a single critical quench, namely an increase of $S(t)$ to a final value which is proportional to the size of the subsystem. On a finer scale, the increase is seen to result from the time evolution within the quench periods which in the simplest case gives a step structure, but becomes partly oscillatory for longer periods and washed out if the dimerization is weak. On the scale of many periods, there are in general oscillations related to the spectrum of the evolution operator. They make the step heights slightly non-uniform and can lead to a striking wave-like approach of S to its asymptotic value. A particularly interesting special case was found for $\delta = 1$ and $\tau = \pi/2$, where the electrons move like massless relativistic particles. This leads to very simple formulae and gives an elementary realization of the picture developed by Calabrese and Cardy for the entanglement process.

We have stressed the close connections to the equilibrium statistics of two-dimensional lattice models. These were also visible in the studies of the kicked Ising chain [6, 7, 8] but, somewhat surprisingly, not pointed out explicitly. The equilibrium models provide a useful reference frame. Thus the concept of the Hamiltonian limit, developed for very anisotropic equilibrium systems, could directly be taken over. On the other hand, the unitary time evolution also introduces some differences. The correlations are typically oscillating and the discrete time intervals between the periods give rise to lattice effects in the frequency domain. The quench could be classified as critical for all values of the period. Any modification in the relative length of the half-periods or in the two dimerizations would lead to gaps in the energies ν_q and thus to a non-critical quench. The entanglement in this case would still show similar overall behaviour due to the quasiparticles in $\bar{H}$ which propagate with the maximum velocity. However, the various band edges in the single-particle dispersions will make the picture more complex in detail. Similarly, a finite quench velocity would complicate matters since in our case one is permanently crossing the quantum critical point $\delta = 0$. The entanglement in such a crossing has so far only been studied for single quenches [34, 35]. There S is not extensive but saturates for large L at a value depending on the transition time. It might be interesting to extend the considerations to the periodic case. In the framework of equilibrium models, this would correspond to a lattice with slowly varying periodic layering.

Note added: A similar situation as studied here was investigated for Heisenberg chains in [36].

Acknowledgement

We would like to thank Thierry Platini and Ulrich Schollwöck for discussions and Peter Barmettler for correspondence.

Appendix: Calculation of the correlation matrix

In this Appendix we summarize the method of obtaining the matrix $\mathbf{C}(t)$ from which the entanglement entropy is calculated for arbitrary dimerizations and quench periods.

In order to calculate the time evolution of the fermionic operators a_j and b_j, it is convenient to switch to the Fourier-transformed operators defined in (2). Then the a_q and b_q evolve for each q independently as

$$\begin{pmatrix} a_q(t) \\ b_q(t) \end{pmatrix} = \begin{pmatrix} \cos\omega_q t & i\mathrm{e}^{-i\varphi_q}\sin\omega_q t \\ i\mathrm{e}^{i\varphi_q}\sin\omega_q t & \cos\omega_q t \end{pmatrix} \begin{pmatrix} a_q \\ b_q \end{pmatrix} = v_q(t) \begin{pmatrix} a_q \\ b_q \end{pmatrix} \tag{30}$$

which is the analogue of (15). In Fourier space, the full evolution matrix always decomposes into such blocks.

During the quench the system is evolved with two different Hamiltonians H_0, H_1 with corresponding matrices $v_{0q}(\tau)$, $v_{1q}(\tau)$ and the time dependent operators after n full periods are given through

$$u_q(2n\tau) = \left[v_{0q}(\tau)v_{1q}(\tau)\right]^n . \tag{31}$$

In order to obtain $u_q(2n\tau)$ one has to raise the matrix $u_q(2\tau)$ to the n-th power, thus one has to determine its eigenvalues and eigenvectors, as well. The eigenvalues can again be written as $\exp(\pm i\gamma_q)$ where

$$\cos\gamma_q = \cos^2\omega_q\tau - \cos(\varphi_1-\varphi_0)\sin^2\omega_q\tau \tag{32}$$

with

$$\cos(\varphi_1-\varphi_0) = \frac{\cos^2(q/2) - \delta^2\sin^2(q/2)}{\cos^2(q/2) + \delta^2\sin^2(q/2)} . \tag{33}$$

To simplify the notation we have dropped the q indices of φ_0 and φ_1. Denoting the first and second component of the i-th eigenvector by A_i and B_i, respectively, the equations then yield

$$|A_{1,2}|^2 = \frac{1}{2}\left[1 \mp \frac{\sin(\varphi_1 - \varphi_0)\sin^2\omega_q\tau}{\sin\gamma_q}\right] \tag{34}$$

and

$$B_{1,2} = \frac{\sin\omega_q\tau\cos\omega_q\tau\,(\mathrm{e}^{i\varphi_1} + \mathrm{e}^{i\varphi_0})}{\pm\sin\gamma_q - \sin(\varphi_1 - \varphi_0)\sin^2\omega_q\tau}\,A_{1,2}\ . \tag{35}$$

With the help of (32)–(35) one can construct the matrix $u_q(2n\tau) = u_q^n(2\tau)$ whose elements read

$$\begin{aligned} u_{11} &= \cos n\gamma_q - i\frac{\sin n\gamma_q}{\sin\gamma_q}\sin(\varphi_1 - \varphi_0)\sin^2\omega_q\tau \\ u_{12} &= i\frac{\sin n\gamma_q}{\sin\gamma_q}\,(\mathrm{e}^{-i\varphi_1} + \mathrm{e}^{-i\varphi_0})\sin\omega_q\tau\cos\omega_q\tau \end{aligned} \tag{36}$$

while the other two elements $u_{21} = -u_{12}^*$ and $u_{22} = u_{11}^*$ follow from unitarity.

Finally, one has to calculate the correlation matrix elements $C_{lj}(2n\tau)$ as defined in (12) which requires knowledge of the initial correlations. These are given as

$$\langle a_q^\dagger a_q\rangle = \langle b_q^\dagger b_q\rangle = 1/2\ , \quad \langle a_q^\dagger b_q\rangle = \langle b_q^\dagger a_q\rangle^* = \mathrm{e}^{i\varphi_0}/2\ . \tag{37}$$

Going over to Fourier transforms and using the form of the evolution matrix $u_q(2n\tau)$ one obtains $C_{lj}(2n\tau) = \frac{1}{2}(\delta_{lj} + \Gamma_{lj})$ with the block matrix

$$\mathbf{\Gamma} = \begin{pmatrix} \Pi_0 & \Pi_{-1} & \cdots & \Pi_{1-N} \\ \Pi_1 & \Pi_0 & & \vdots \\ \vdots & & \ddots & \vdots \\ \Pi_{N-1} & \cdots & \cdots & \Pi_0 \end{pmatrix}\ , \qquad \Pi_m = \begin{pmatrix} f_m & g_m \\ g_{-m}^* & -f_m \end{pmatrix} \tag{38}$$

where $m = l - j$ and the matrix elements of the 2×2 matrices Π_m read in the thermodynamic limit

$$\begin{aligned} f_m &= \int_{-\pi}^{\pi}\frac{\mathrm{d}q}{\pi}\mathrm{Re}\left(u_{22}u_{12}\mathrm{e}^{i\varphi_0}\right)\mathrm{e}^{-iqm}\ , \\ g_m &= \int_{-\pi}^{\pi}\frac{\mathrm{d}q}{2\pi}\left(u_{22}^2\mathrm{e}^{i\varphi_0} - u_{21}^2\mathrm{e}^{-i\varphi_0}\right)\mathrm{e}^{-iqm}\ . \end{aligned} \tag{39}$$

Up to now we have considered only the special time instances $t_n = 2n\tau$. To extend the calculation to arbitrary times $t_n < t < t_{n+1}$ one has to calculate the matrix elements of

$$u_q(t) = \begin{cases} v_{1q}(t - t_n)\,u_q(t_n), & \text{if } t < t_n + \tau \\ v_{0q}^+(t_{n+1} - t)\,u_q(t_{n+1}), & \text{if } t \geq t_n + \tau \end{cases} \tag{40}$$

and substitute them in (39) to obtain the matrix $\mathbf{\Gamma}$ for intermediate times.

It is also interesting to investigate the asymptotic ($n \to \infty$) behaviour of the matrix elements. Then the integrals in (39) have rapidly oscillating arguments, and one can replace $\cos n\gamma_q$ and $\sin n\gamma_q$ by zero as well as $\cos^2 n\gamma_q$ and $\sin^2 n\gamma_q$ by 1/2, as these factors are multiplied by smooth functions of q and integrated over. After a lengthy calculation one has the form

$$\begin{aligned} f_m(\infty) &= \int_{-\pi}^{\pi} \frac{\mathrm{d}q}{2\pi} \frac{i \sin\omega_q\tau\cos\omega_q\tau}{\delta^2\tan^2\frac{q}{2} + \cos^2\omega_q\tau} \delta \tan\frac{q}{2} \sin qm \,, \\ g_m(\infty) &= \int_{-\pi}^{\pi} \frac{\mathrm{d}q}{2\pi} \frac{\omega_q \cos^2\omega_q\tau}{\delta^2\tan^2\frac{q}{2} + \cos^2\omega_q\tau} (\cos qm + \tan\frac{q}{2}\sin qm) \,. \end{aligned} \tag{41}$$

For $\delta = 1$ and $\tau \to 0$ all expressions simplify considerably. Then f_m and g_m become Bessel functions and their asymptotic values are $f_m(\infty) = 0$ and $g_m(\infty) = (\delta_{m,0} + \delta_{m,1})/2$. This gives the correlation matrix found in [31] for a single quench.

[1] L. Amico, R. Fazio, A. Osterloh, and V. Vedral, preprint quant-ph/0703044 (2007).

[2] P. Calabrese and J. L. Cardy, J. Stat. Mech. P04010 (2005).

[3] G. De Chiara, S. Montangero, P. Calabrese, and R. Fazio, J. Stat. Mech. P03001 (2006).

[4] N. Schuch, M. M. Wolf, K. G. H. Vollbrecht, and J. I. Cirac, eprint arXiv:0801.2078 (2008).

[5] A. M. Läuchli and C. Kollath, eprint arXiv:0803.2947 (2008).

[6] T. Prosen, Progr. Theor. Phys. Supplement **139**, 191 (2000).

[7] A. Lakshminarayan and V. Subrahmanyam, Phys. Rev. A **71**, 062334 (2005).

[8] J. P. Barjaktarevic, G. J. Milburn, and R. H. McKenzie, Phys. Rev. A **71**, 012335 (2005).

[9] T. Prosen, Phys. Rev. E **65**, 036208 (2002).

[10] T. Prosen, J. Phys. A **40**, 7881 (2007).

[11] M. Saunders, P. L. Halkyard, K. J. Challis, and S. A. Gardiner, Phys. Rev. A **76**, 043415 (2007), and references therein.

[12] T. Stöferle, H. Moritz, C. Schori, M. Köhl, and T. Esslinger, Phys. Rev. Lett. **92**, 130403 (2004).

[13] C. Schori, T. Stöferle, H. Moritz, M. Köhl, and T. Esslinger, Phys. Rev. Lett. **92**, 240402 (2004).

[14] A. Iucci, M. A. Cazalilla, A. F. Ho, and T. Giamarchi, Phys. Rev. A **73**, 041608(R) (2006).

[15] C. Kollath, A. Iucci, T. Giamarchi, W. Hofstetter, and U. Schollwöck, Phys. Rev. Lett. **97**, 050402 (2006).

[16] C. Kollath, A. Iucci, I. McCulloch, and T. Giamarchi, Phys. Rev. A **74**, 041604(R) (2006).

[17] S. Dorosz, T. Platini, and D. Karevski, preprint arXiv:0709.2637 (2007).

[18] F. Haake, Quantum Signatures of Chaos, 2nd edition (Springer, Berlin, 2000).

[19] I. Peschel, J. Phys. A **36**, L205 (2003).

[20] T. D. Schultz, D. C. Mattis, and E. H. Lieb, Rev. Mod. Phys. **36**, 856 (1964).

[21] L. Turban, Phys. Lett. A **104**, 435 (1984).

[22] I. Peschel and K. D. Schotte, Z. Phys. B **54**, 305 (1984).

[23] F. Iglói and R. Juhász, Europhys. Lett. **81**, 57003 (2008).

[24] V. Eisler, D. Karevski, T. Platini, and I. Peschel, J. Stat. Mech. P01023 (2008).

[25] O. Romero-Isart and J. J. García-Ripoll, Phys. Rev. A **76**, 052304 (2008).

[26] D. Kandel, E. Domany, and B. Nienhuis, J. Phys. A **23**, L755 (1990).

[27] G. Schütz, Phys. Rev. E **47**, 4265 (1993).

[28] A. Honecker and I. Peschel, J. Stat. Phys. **88**, 319 (1997).

[29] H. N. V. Temperley and E. H. Lieb, Proc. Roy. Soc. London **322**, 251 (1971).

[30] F. F. Assaad and H. G. Everts, in: Computational Many-Particle Physics, H. Fehske, R. Schneider, and A. Weisse (eds.), Lecture Notes in Physics, vol. 739 (Springer, Berlin, 2008), pp. 277-356.

[31] V. Eisler and I. Peschel, J. Stat. Mech. P06005 (2007).

[32] J. Eisert and T. J. Osborne, Phys. Rev. Lett. **97**, 150404 (2006).

[33] S. Bravyi, M. B. Hastings, and F. Verstraete, Phys. Rev. Lett. **97**, 050401 (2006).

[34] R. W. Cherng and L. S. Levitov, Phys. Rev. A **73**, 043614 (2006).

[35] L. Cincio, J. Dziarmaga, M. M. Rams, and W. H. Zurek, Phys. Rev. A **75**, 052321 (2007).

[36] P. Barmettler, A. M. Rey, E. Demler, M. D. Lukin, I. Bloch, and V. Gritsev, preprint arXiv:0803.1643 (2008).